

Tubular Links for Eccentrically Braced Frames. I: Finite Element Parametric Study

Jeffrey W. Berman¹ and Michel Bruneau²

Abstract: This paper describes the development and results of a finite element parametric study of eccentrically braced frame links having hollow rectangular cross sections (i.e., tubular links). The parametric study involves over 200 combinations of geometries and properties and is divided into two parts. Part A considers a wide range of compactness ratios and link lengths to determine appropriate compactness ratio limits such that links with tubular cross sections can achieve desired rotation levels prior to significant strength degradation from local buckling. Part B of the study involves models developed with flange compactness ratios, web compactness ratios, and stiffener spacings near the proposed design limits from Part A, and also examines links having webs and flanges with different yield stresses (i.e., hybrid links). Results of the parametric study are also used to investigate the adequacy of a method for approximating link overstrength. A companion paper describes the experimental verification of the proposed design requirements.

DOI: 10.1061/(ASCE)0733-9445(2008)134:5(692)

CE Database subject headings: Seismic design; Steel structures; Ductility; Rotation; Finite element method; Steel frames; Bracing.

Introduction

Eccentrically braced frames (EBFs), which rely on yielding of a link beam between braces, have been shown to provide ductility and energy dissipation under seismic loading (Roeder and Popov 1978a,b; Popov and Bertero 1980; Hjelmstad and Popov 1983; 1984; Malley and Popov 1984; Kasai and Popov 1986a,b; Ricles and Popov 1989; Engelhardt and Popov 1992, among others). Guidelines for EBF design with links having wide-flange (WF) cross sections are in the current AISC seismic provisions (AISC 2005). However, the use of WF shapes as link beams necessitates that they be braced out-of-plane to prevent lateral torsional buckling. This requirement has limited their use in bridge piers where lateral bracing is difficult to provide.

There have been some applications of EBFs with built-up I-shaped links in bridge piers for long span bridges such as the San Francisco-Oakland Bay Bridge and the Richmond-San Rafael Bridge (Dusicka et al. 2002; Itani 1997). In these cases, either very short links were used or special considerations for link stability were made, which may have increased the cost of the projects. Therefore, the development of a link type that does not require lateral bracing is desirable for application of EBFs in bridge piers. Such self-stabilizing links would also be useful in

buildings where lateral bracing may not be feasible or easily provided, such as in an elevator core area where floor framing is not present. Further, the design of EBFs to protect existing bridge pier bracing members may be employed using the approach in Berman and Bruneau (2005b), or EBF systems may be used to replace existing deficient pier brace systems.

A proof-of-concept EBF having a link with a tubular cross section and no lateral bracing has been tested and shown to possess ductility and rotation capacity similar to that of WF links (Berman and Bruneau 2007). Tubular cross sections, such as the general one shown in Fig. 1, have substantial torsional stability, making them less susceptible to lateral torsional buckling, thereby reducing or eliminating the need for lateral bracing. On the strength of this successful proof-of-concept test, it is desirable to develop design recommendations for tubular cross sections employed in this application. Of primary importance is the development of limit compactness ratios for the webs and flanges as well as minimum stiffener requirements such that links can achieve desired rotation levels prior to strength degradation from local buckling. It is also important to characterize the expected overstrength of tubular links with various cross-sectional properties so that capacity design of surrounding framing may be achieved. Further, as tubular links may be built-up or hybrid cross sections consisting of webs and flanges with differing thicknesses and yield strengths, the proposed compactness ratio limits must be applicable for a range of yield stresses. Note that built-up sections are considered because the longest shear link possible with a common HSS is 457 mm (Berman and Bruneau 2005a). This is a rather short length and will result in large rotation demands at design frame drift levels. Therefore, built-up tubular links are likely necessary and are the subject of this research.

This paper describes a finite element parametric study, aimed at determining limiting compactness ratios for EBF links having tubular cross sections, involving over 200 combinations of geometries and material properties. First, a finite element model of the link from proof-of-concept testing in Berman and Bruneau (2007) is briefly discussed as this is the base model for the parametric study. Following this, the parametric study is presented in two

¹Assistant Professor, Dept. of Civil and Environmental Engineering, More Hall 201-Box 352700, Univ. of Washington, Seattle, WA 98195-2700. E-mail: jwberman@u.washington.edu

²Director, Multidisciplinary Center for Earthquake Engineering Research, Professor, Dept. of Civil Structural and Environmental Engineering, Univ. at Buffalo, Amherst, NY 14260. E-mail: bruneau@mceermail.buffalo.edu

Note. Associate Editor: Benjamin W. Schafer. Discussion open until October 1, 2008. Separate discussions must be submitted for individual papers. To extend the closing date by one month, a written request must be filed with the ASCE Managing Editor. The manuscript for this paper was submitted for review and possible publication on June 15, 2006; approved on April 9, 2007. This paper is part of the *Journal of Structural Engineering*, Vol. 134, No. 5, May 1, 2008. ©ASCE, ISSN 0733-9445/2008/5-692-701/\$25.00.

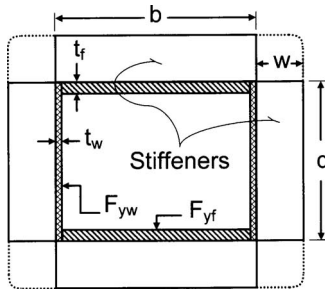


Fig. 1. Generic tubular cross section with perimeter stiffeners

parts. Part A considers a wide range of compactness ratios and link lengths to develop proposed design requirements. Part B of the study involves models developed with flange compactness ratios, web compactness ratios, and stiffener spacings near the proposed design limits, and also examines links having webs and flanges with different yield stresses (i.e., hybrid links). Results from both parts of the study are also used to adapt a link overstrength formulation by Richards (2004) for WF links to links having tubular cross sections. The companion paper, Berman and Bruneau (2007b), describes the experimental verification of the proposed design requirements using 14 different test specimens.

It is important to note that this parametric study parallels a similar analytical study of the effect of flange width-to-thickness ratio on WF EBF link rotation capacity by Richards and Uang (2005), which also considered experimental data from Okazaki et al. (2005, 2006). As discussed herein, similar analytical models and failure criteria are chosen for the current study for the purpose of maintaining consistency such that implementation of links with tubular cross sections may be efficiently achieved.

Finite-Element Modeling of Proof-of-Concept Link

A finite element model of the link from the EBF proof-of-concept testing reported on in Berman and Bruneau (2007) was developed using the software package ABAQUS (HKS 2001). This model was developed using four-node reduced integration shell elements and employed nonlinear material and geometry. The details of the tested link are shown in Figs. 2 and 3 and the link sustained a full-cycle at a maximum rotation of 0.123 rad, over 50% more than the maximum rotation of 0.08 rad allowed for design of shear links with WF cross sections.

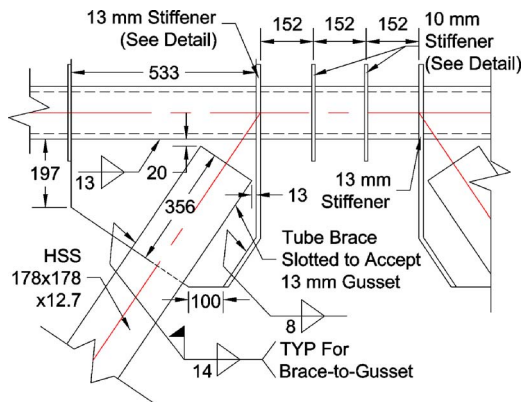


Fig. 2. Proof-of-concept link details

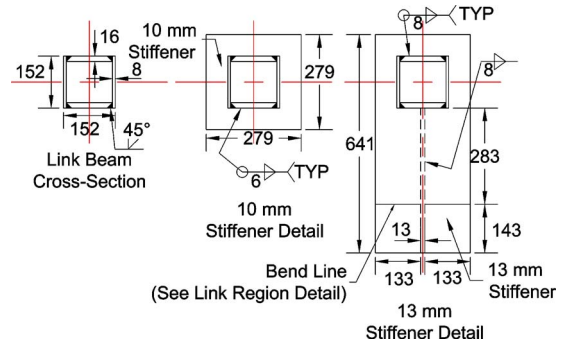


Fig. 3. Proof-of-concept link cross sections

The material model selected had only kinematic hardening, i.e., it neglected the isotropic hardening component which is acceptable for steel at large strains (Berman and Bruneau 2006), and was based on cyclic coupon test results of the web and flange material. The boundary conditions used are shown in Fig. 4 and were the same boundary conditions used by Richards and Uang (2005) in their study of WF links. These boundary conditions ensure that equal link end moments are obtained and also prevent the development of link axial force. Loading was applied as a vertical displacement at the right end of the link and the rotation history from the link of the proof-of-concept test was used, which complied with ATC-24 (ATC 1992). This loading protocol was selected for the proof-of-concept test because system behavior, rather than just link behavior, was being explored. The ATC-24 protocol is based on a system yield displacement as opposed to a link rotation and therefore seemed to be the appropriate protocol for this test. A mesh refinement study was performed to determine the adequate mesh density for the finite elements. A comparison of the simulated and experimentally obtained link deformed shapes are shown in Fig. 5 for the final mesh, which had element width-to-thickness ratios in the range of 1.6–3.5. Comparing the link shear force versus rotation hysteresis curves in Fig. 6 shows reasonable agreement with the experimental results. Note that residual stresses were not considered in the modeling, although they should only effect the initial yielding.

Finite-Element Parametric Study

Using the finite element model of the link from the proof-of-concept test as a basis, a parametric study of tubular links was performed. The parametric study consisted of two parts: Part A investigated links with a wide range of web and flange compactness ratios to assess the adequacy of the derived flange compactness ratio limit and stiffener spacing equation from Berman and Bruneau (2007), and the results are used to modify those local

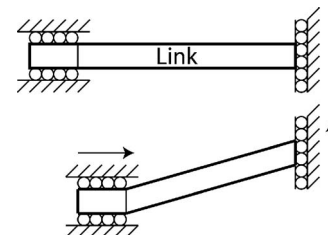
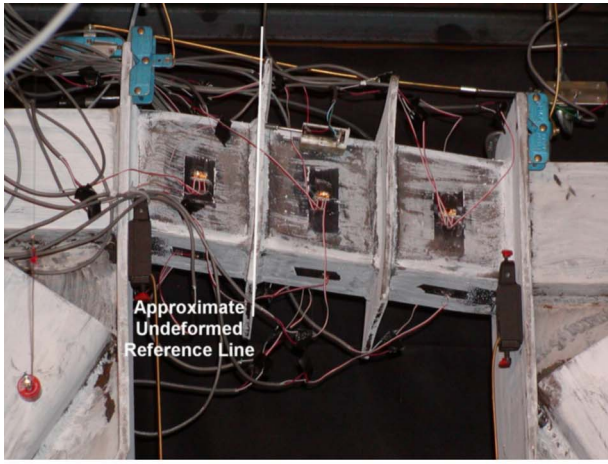
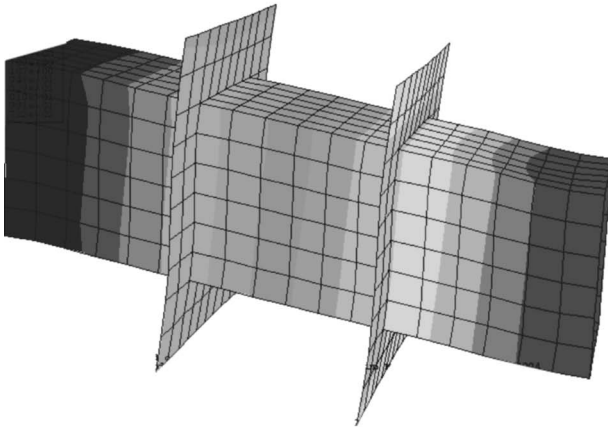


Fig. 4. Finite-element model boundary conditions



(a)



(b)

Fig. 5. Comparison of proof-of-concept link deformations: (a) experimental; (b) finite-element model

buckling prevention criteria as necessary; Part B examined a range of web and flange yield stresses for links with webs and flanges having compactness ratios close to the modified limits. Both parts of the parametric study had links with normalized lengths, ρ , corresponding to shear, intermediate, and flexural links, where

$$\rho = \frac{e}{(M_p/V_p)} \quad (1)$$

M_p and V_p =plastic moment and shear capacity of the cross section and e =link length. The normalized link lengths representing the transitions from shear-to-intermediate and intermediate-to-flexural links are 1.6 and 2.6, respectively, which are the same transition lengths currently used for links with WF cross sections (AISC 2005). The plastic shear and moment capacities of the tubular links are (Berman and Bruneau 2007)

$$V_p = \frac{2}{\sqrt{3}} F_{yw} t_w (d - 2t_f) \quad (2)$$

$$M_p = F_{yf} t_f (b - 2t_w)(d - t_f) + F_{yw} \frac{t_w d^2}{2} \quad (3)$$

where F_{yw} , t_w , and d =web yield strength, web thickness, and web depth, respectively, and F_{yf} , t_f , and b =flange yield strength, flange width, and flange thickness, respectively.

Parametric Study Part A: Setup

Four parameters were used to develop the links in Part A of the parametric study: normalized link length, ρ , flange compactness ratio, b'/t_f (where $b'=b-2t_w$), web compactness ratio, d'/t_w (where $d'=d-2t_f$), and stiffener spacing, a . A total of 64 stiffened and 64 unstiffened links with various cross sections and lengths were analyzed, as described in the following. Note that web and flange thicknesses of 8 and 18 mm, respectively, were used for all models and the web and flange widths were varied to give the selected compactness ratios. For the purpose of nomenclature, links will be labeled using S or N (for stiffened or unstiffened) followed by the numerical values for the parameters b'/t_f , d'/t_w , and ρ . For example, the name N-8-12-1.6 refers to an unstiffened link with a flange compactness of 8, web compactness of 12, and normalized length of 1.6.

Three normalized link lengths representing shear, intermediate, and flexural links were selected, namely, $\rho=1.2$, 2.1, and 3.0, as they represent evenly spaced values of normalized link lengths well within all three ranges of expected behavior (delineated by the transition points of $\rho=1.6$ and $\rho=2.6$ as indicated earlier). In addition, the length $\rho=1.6$ was selected to verify that the proposed design rules work at this important transition length. The target plastic rotations, γ_p , for the links considered are 0.08 rad for $\rho=1.2$ and 1.6, and 0.05 and 0.02 rad for links with $\rho=2.1$ and 3.0, respectively. These target rotations are the maximum rotations allowed for WF links in the AISC Seismic Provisions.

Flange compactness ratios were selected so that the applicability of the derived limit from Berman and Bruneau (2007a) and the limit in the AISC Seismic Provisions for tubular sections used as brace members could be evaluated. The limit from Berman and Bruneau (2007a) is

$$b'/t_f \leq 1.02 \sqrt{E_s F_{yf}} \quad (4)$$

where E_s =modulus of elasticity for steel and F_{yf} =flange yield strength. The AISC limit for tubular cross sections is

$$b'/t_f \leq 0.64 \sqrt{E_s F_{yf}} \quad (5)$$

For $F_{yf}=345$ MPa and $E_s=2 \times 10^5$ MPa, which are the values used in the Part A models (see the following), the flange compactness ratio limit from Berman and Bruneau is 24.5 and the AISC limit is 15.4. It is also desirable to have information on links with

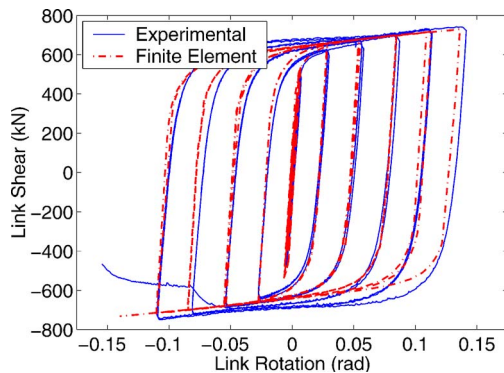


Fig. 6. Comparison of analytical and experimental link shear versus rotation hysteresis curves

Table 1. Cross-Section Dimensions for Part A Links

b'/t_f	8.0	17.0	24.0	40.0
b' (mm)	127	270	381	635
b (mm)	143	286	397	651
No. elements	5	11	15	25
El. elements	5	11	15	25
El. edge-to-thickness ^a	1.6	1.5	1.6	1.6
d'/t_w	12.0	16.0	24.0	36.0
d' (mm)	95	127	191	286
d (mm)	127	159	222	318
No. elements	4	6	8	12
El. edge-to-thickness ^a	3.0	2.7	3.0	3.0

^aThe mesh refinement study during proof-of-concept link modeling indicated values between 1.6 and 3.2 gave acceptable results (Berman and Bruneau 2007).

relatively stocky and slender flanges to examine the effect of link overstrength and the general effect of flange compactness on link behavior. Therefore, flange compactness ratios of 8.0, 17.0, 24.0, and 40.0 were selected, the first being well below both limits, the second near the AISC limit, the third near the derived limit, and the fourth well above both limits.

Limits for webs of HSS shapes in the AISC seismic provisions are the same as those for the flanges, i.e., $d'/t_w \leq 0.64\sqrt{E_s/F_{yw}}$. However, this limit was found for HSS sections in compression, and larger compactness ratios may be possible here as the link webs yield in shear and may have stiffeners. Therefore, webs compactness ratios below and well above that limit were selected and both stiffened and unstiffened cases were considered. The web compactness ratios selected were 12.0, 16.0, 24.0, and 36.0. For links with stiffeners, the stiffener spacing was selected to satisfy the equation for tubular links as derived in Berman and Bruneau (2007)

$$\frac{a}{t_w} + \frac{1}{8} \frac{d}{t_w} = C_B \quad (a \leq d) \quad (6)$$

where $C_B=20$ and 37 for ultimate link rotations of 0.08 and 0.02 rad, respectively. Note that for a web compactness ratio of 36, the required stiffener spacing, a , found from the proposed stiffener spacing equation is 0.43 times the web depth d , which is near a practical lower bound on stiffener spacing. When rounding of the stiffener spacing obtained from Eq. (6) was necessary to conform with the element mesh, it was done such that the spacing at the link ends was always greater than the result from Eq. (6) to ensure conservative results. Stiffener widths and thicknesses were selected according to the requirements derived in Berman and Bruneau (2007).

As mentioned earlier, all link models in Part A of the parametric study had web and flange thicknesses of 8 and 16 mm, respectively. Using these thicknesses, the above-discussed compactness ratios, and nominal yield stresses and moduli of elasticity for both the webs and flanges of 345 MPa and 2×10^5 MPa, respectively, the link cross-section dimensions given in Table 1 were calculated. The resulting cross-section aspect ratios, b/d , are shown in Table 2. Note that all link models had element width-to-thickness ratios comparable to that used for the final mesh refinement of the proof-of-concept link model as shown in Table 1.

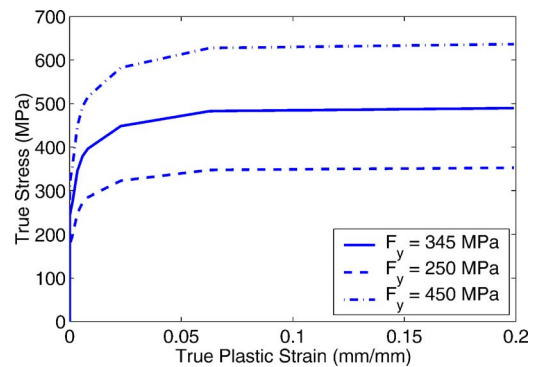
Two differences between the link models of the parametric study and the model of the proof-of-concept link were used, namely, the input data for the material model and the loading

Table 2. b/d Ratios for Part A Link

d'/t_w	b'/t_f			
	8.0	17.0	24.0	40.0
12.0	1.13	2.25	3.13	5.13
16.0	0.90	1.80	2.50	4.10
24.0	0.64	1.29	1.79	2.93
36.0	0.45	0.90	1.25	2.05

history. The material data used as input for the kinematic hardening material model for the links of Part A of the finite element parametric study are shown as the solid true stress versus true strain curve in Fig. 7. These data differ from that used in the model of the proof-of-concept link, which was based on coupon test results for that link's steel. The data used in the parametric study are based on cyclic coupon test results for A572 Grade 50 steel from Kaufmann et al. (2001). The loading history used for the parametric study links was that given for link testing in the 2002 AISC Seismic Design Provisions for Steel Buildings (AISC 2002), which specifies three cycles at each total link rotation level of 0.0025, 0.005, and 0.01 rad, followed by two cycles at 0.01 rad increments up to the maximum code specified rotation. However, for the current research purposes, loading was continued with two cycles at 0.01 rad increments up to 0.2 rad of total rotation or convergence failure due to very large buckling displacements, whichever happened first. Note that a revision to this loading protocol now appears in the 2005 AISC Seismic Design Provisions for Steel Buildings (AISC 2005) and it has been shown that the older loading is more severe and therefore conservative (Okazaki et al. 2005; Richards and Uang 2006; Berman and Bruneau 2008).

For the purpose of this parametric study, the limit plastic rotation, γ_{lim} , is defined as the inelastic rotation at which the backbone curve of the link shear force hysteresis drops below 80% of the maximum link shear force obtained for a given link. This definition is selected because it represents a negligible degradation so that a bilinear approximation may be used in practice and it is also consistent with what has been done for WF links. The procedure used here to determine the limit rotation is similar to

**Fig. 7.** True stress versus true strain curves for finite element parametric study

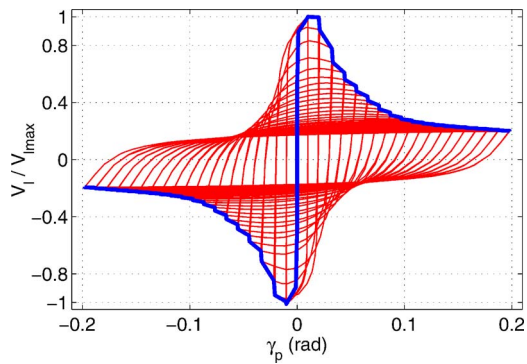


Fig. 8. Example of limit plastic rotation determination.

that used by Richards and Uang (2005) in their study of over-strength and rotation capacity of WF links and can be described as follows.

First, the normalized link shear force versus plastic rotation hysteresis curve was calculated using MATLAB (Math Works 1999) and the results from ABAQUS. For each link, the initial stiffness, k_{li} , was determined by fitting a line through the first three points of the link shear versus total rotation hysteresis curve. The plastic rotation at any point in the load history, γ_p , is then determined from

$$\gamma_p = \gamma_t = -\frac{V_l}{k_{li}} \quad (7)$$

where γ_t = total rotation and V_l = link shear. The shear force, V_l , is then normalized by the maximum link shear, $V_{l,max}$, obtained for each link.

From the normalized link shear versus plastic rotation hysteresis, the backbone curve is constructed and a simple search algorithm is used to find the limit plastic rotation, $\gamma_{p,lim}$, where the link shear force drops below 80% of the maximum. This limit is selected because it has been used in other similar studies regarding plastic rotation capacity since its recommendation in SAC (1997). An example is shown in Fig. 8 for an unstiffened link with flange and web compactness ratios of 24 and a normalized link

length of 2.1, for which the limit plastic rotation was found to be 0.0325 rad. Note that in the companion paper, Berman and Bruneau (2008), only one of the links tested suffered severe local buckling and corresponding strength degradation prior to fracture as shown in Fig. 8. Therefore, severe local buckling in the analytical models has only been verified for that single data point, for which the analytically obtained hysteresis shape, energy dissipation, and limit plastic rotation are shown to agree favorably with experimental results (Berman and Bruneau 2008). Further, the study by Richards and Uang (2005) used similar shell element models of WF links and their results were shown to agree favorably with test results from Okazaki et al. (2005).

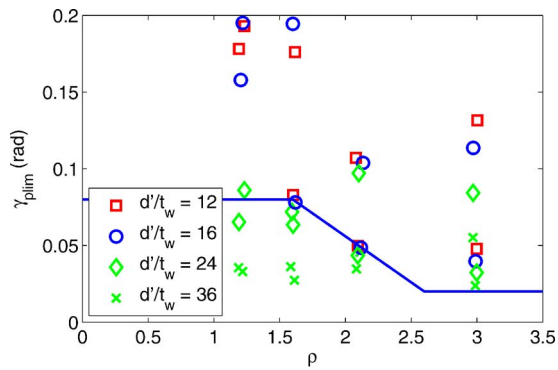
Parametric Study Part A: Results

The limit plastic rotation obtained for the link analyses in Part A of the parametric study are given in Table 3. Recall that no attempt to model fracture was made and therefore some of the links that have large limit plastic rotations might, in practice, fracture prior to reaching those plastic rotations. For example, the proof-of-concept specimen fractured at a total rotation of 0.15 rad yet the finite element results for that specimen would indicate that a plastic rotation greater than 0.2 rad could be achieved prior to strength degradation from buckling.

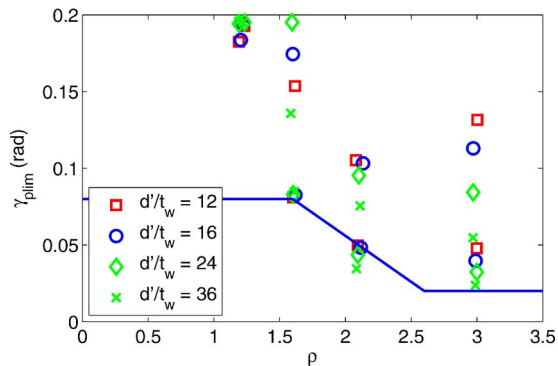
Several observations can be made regarding the effect of stiffeners and web compactness on a link's ability to reach the target rotation by plotting the data from Table 3 as a function of normalized link length for links with $b'/t_f \leq 17.0$ and grouping results in terms of d'/t_w values, as shown in Figs. 9(a and b). For reference, these figures also have a solid line indicating the AISC specified maximum rotation (also referred to as the target rotation). First, it appears that links with $d'/t_w \leq 16.0$ and $b'/t_f \leq 17.0$ can achieve their target rotation without stiffeners. These are shown as the squares ($d'/t_w = 12.0$) and circles ($d'/t_w = 16.0$) of Fig. 9(a). It was shown by Berman and Bruneau (2005a) that the theoretical stiffener spacing equation, for which Eq. (6) is a convenient approximation, indicates that no stiffeners would be required for webs with compactness ratios of less than 17.0 (the current AISC compactness limit is 15.4 for rectangular HSS with

Table 3. Limit Plastic Rotations for Part A Links (rad)

b'/t_f	d'/t_w	Unstiffened				Stiffened			
		$\rho=1.2$	$\rho=1.6$	$\rho=2.1$	$\rho=3.0$	$\rho=1.2$	$\rho=1.6$	$\rho=2.1$	$\rho=3.0$
8.0	12.0	0.193	0.176	0.107	0.132	0.193	0.154	0.105	0.132
8.0	16.0	0.195	0.195	0.104	0.114	0.194	0.174	0.103	0.113
8.0	24.0	0.086	0.072	0.097	0.084	0.195	0.195	0.095	0.084
8.0	36.0	0.036	0.036	0.046	0.055	0.196	0.136	0.076	0.055
17.0	12.0	0.178	0.083	0.049	0.048	0.182	0.081	0.050	0.048
17.0	16.0	0.158	0.078	0.049	0.040	0.184	0.083	0.048	0.040
17.0	24.0	0.065	0.064	0.044	0.032	0.194	0.083	0.044	0.032
17.0	36.0	0.033	0.027	0.035	0.024	0.195	0.085	0.035	0.024
24.0	12.0	0.122	0.050	0.040	0.044	0.117	0.059	0.043	0.036
24.0	16.0	0.123	0.051	0.030	0.028	0.119	0.071	0.035	0.028
24.0	24.0	0.058	0.049	0.033	0.027	0.154	0.056	0.034	0.027
24.0	36.0	0.026	0.032	0.024	0.021	0.194	0.064	0.024	0.020
40.0	12.0	0.067	0.026	0.033	0.019	0.092	0.044	0.022	0.020
40.0	16.0	0.060	0.030	0.017	0.028	0.107	0.047	0.033	0.030
40.0	24.0	0.063	0.033	0.023	0.019	0.100	0.044	0.020	0.019
40.0	36.0	0.032	0.024	0.013	0.011	0.118	0.054	0.023	0.013



(a)



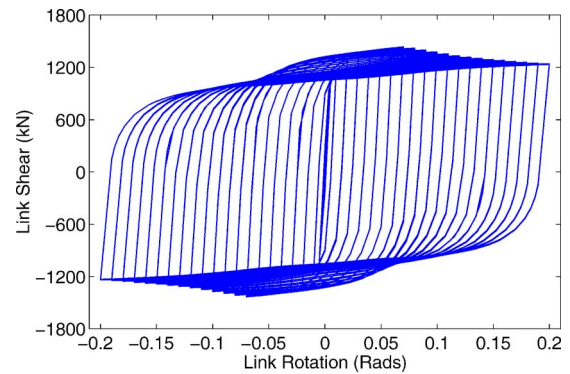
(b)

Fig. 9. Limit plastic rotations for Part A links with $b'/t_f \leq 17$: (a) unstiffened; (b) stiffened

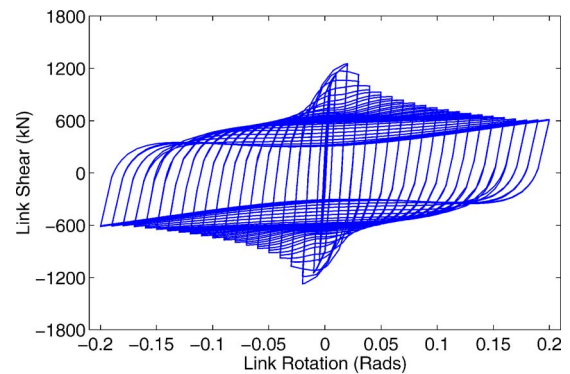
$F_{yw}=345$ MPa). Therefore, the results of the analyses seem to validate this prediction, as long as the flange compactness ratio is also kept less than or equal to 17.0. There are three exceptions to this, namely, N-17-16-1.6, N-17-12-2.1, and N-17-16-2.1, which are discussed further in the following.

The results in Table 3 also indicate that stiffeners were effective in helping shear links with web compactness ratios up to 36.0 and flange compactness ratios less than or equal to 17.0 achieve the target rotation. For instance, the limit plastic rotation for S-17-36-1.2 was 0.195 rad and the hysteresis was full and stable as shown in Fig. 10(a), whereas without stiffeners the limit plastic rotation for that same link (N-17-36-1.2) was 0.033 rad and the hysteresis showed rapid strength degradation following web buckling at small plastic rotations as shown in Fig. 10(b). This is demonstrated further in Figs. 9(a and b). Note that the web compactness of 36.0 corresponds to $d'/t_w = 1.50\sqrt{E_s/F_{yw}}$ with $F_{yw}=345$ MPa and $E_s=2 \times 10^5$ MPa, which will be used later to develop dimensionless compactness limits.

For intermediate and flexural links, there was little difference in limit plastic rotation obtained between stiffened and unstiffened links because flange buckling occurred between stiffeners. N-8-36-2.1 was the only intermediate link for which the addition of stiffeners was found to help it reach and exceed the target rotation. As this link had a low flange compactness ratio and high web compactness ratio, web buckling was the trigger for strength degradation. When stiffeners were added, web buckling (and the corresponding strength degradation due to web buckling) was delayed and the link achieved a 0.076 rad rotation prior to a 20% strength degradation that was initiated by flange buckling. For the other intermediate and flexural links considered, flange buckling was the trigger for strength degradation and the addition of stiff-



(a)



(b)

Fig. 10. Link shear versus rotation hysteresis curves for (a) S-17-36-1.2; (b) N-17-36-1.2

eners did not effectively delay this buckling mode. However, intermediate and flexural links with a given value of flange compactness exhibited decreasing limit plastic rotations with increasing web compactness ratios, indicating that the stabilizing effect of the web against flange buckling decreases with increasing web compactness ratios. From the cases considered, it also appears that flexural links with web compactness up to 36.0 can reach their target rotation as long as the flange compactness is less than or equal to 24.0.

Figs. 11(a and b) show limit plastic rotation versus link length for stiffened and unstiffened links, respectively, both with $b'/t_f > 17.0$. When comparing these with Figs. 9(a and b), which showed the same information for links with $b'/t_f \leq 17.0$, it is observed that many links with larger flange compactness ratios did not achieve their target rotation. Comparing Figs. 11(a and b) with Figs. 9(a and b) also shows that stiffeners improved the rotation capacity of all shear links, however, only for links with $b'/t_f \leq 17.0$ was that improvement enough to reach the target rotation of 0.08 rad for both $\rho=1.2$ and 1.6. Additionally, only stiffened shear links with $\rho=1.2$ were able to consistently meet their target rotation when $b'/t_f > 17.0$. At the transition length from shear to intermediate links, $\rho=1.6$, and at the intermediate length of $\rho=2.1$, no links with $b'/t_f > 17.0$ achieved the target rotation, even when stiffened. Further, proving stiffeners for links where flange buckling was critical (i.e., links with $\rho \geq 2.1$ and $b'/t_f > 17.0$) appeared to have little effect on flange buckling, as seen by examining unstiffened sections with $b'/t_f > 17.0$, which had similar limit plastic rotations to those same sections with stiffeners. Therefore, stiffeners need not be connected to the flange as long as $b'/t_f \leq 17.0$.

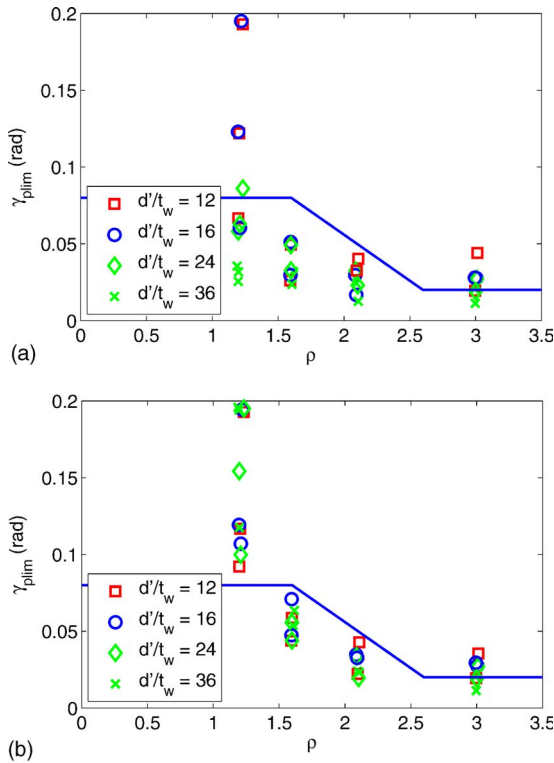


Fig. 11. Limit plastic rotations for Part A links with $b'/t_f > 17$: (a) unstiffened; (b) stiffened

The three unstiffened links, namely, N-17-12-2.1, N-17-16-1.6, and N-17-16-2.1, that had $b'/t_f \leq 17.0$ along with $b'/t_w \leq 16.0$ and did not reach their target rotation were investigated in more detail. Flange buckling was the trigger for strength degradation and they all came to within 3% of their target rotations, which could be considered insignificant for engineering purposes. However, for completeness, as the AISC limit for flange compact-

ness is actually 15.4 for $F_{yf} = 345$ MPa (50 ksi) and a value of 17.0 had been used to develop the models, these three links were reanalyzed with a modified flange thickness corresponding to a flange compactness of 15.9 (a value slightly larger than 15.4 was selected to be conservative). The limit plastic rotations for these modified links were found to be 0.051, 0.083, and 0.050 rad, respectively, which are greater than or equal to their target rotations.

Design Recommendations

Based on the results of Part A of the finite element parametric study and the above-presented discussion, recommended compactness ratio limits for tubular links are given and compared to AISC limits for rectangular HSS shapes and the limits derived in Berman and Bruneau (2007), which were summarized at the beginning of this paper. This comparison of compactness ratio limits is shown in Table 4. Note that the recommended stiffened web compactness ratio limit for shear links based on the parametric study results is $1.67\sqrt{E_s/F_{yw}}$. In Part A of the parametric study a web yield stress of 345 MPa and d'/t_w of 36 were used. This d'/t_w value was determined based on limiting the minimum stiffener spacing, a , to approximately $0.4d'$, considered to be a practical minimum. Substituting this stiffener spacing into Eq. (6) with $C_B = 20$, which is the value for shear links with an anticipated rotation of 0.08 rad, gives the d'/t_w value of 36. The web compactness ratio that corresponds to this yield strength and d'/t_w value is $1.50\sqrt{E_s/F_{yw}}$. The larger value of $1.67\sqrt{E_s/F_{yw}}$ recommended in Table 4 has been determined from ancillary models not presented here that considered a web yield stress of 1.25 times the 345 MPa yield stress used in Part A. These case studies revealed that stiffened shear links with this web compactness ratio and web yield stress could achieve their target rotation. Part B of the parametric study will focus on investigating the appropriateness of the proposed limit for various steel yield strengths.

It is also recommended, based on the results of Part A of the parametric study, that web compactness ratios for intermediate

Table 4. Compactness Limit Comparison

Link category	Compactness ratio	Current AISC limits	Limits derived in Berman and Bruneau (2007a)	Limits based on Part A FE results
Shear links	b'/t_f	$0.64\sqrt{E_s/F_{yf}}$	$1.02\sqrt{E_s/F_{yf}}$	$0.64\sqrt{E_s/F_{yf}}$
	Stiffened d'/t_w	^a	^b	$1.67\sqrt{E_s/F_{yw}}$ ^c
	Unstiffened d'/t_w	$0.64\sqrt{E_s/F_{yw}}$	^b	$0.64\sqrt{E_s/F_{yw}}$
Intermediate links	b'/t_f	$0.64\sqrt{E_s/F_{yf}}$	$1.02\sqrt{E_s/F_{yf}}$	$0.64\sqrt{E_s/F_{yf}}$
	Stiffened d'/t_w	^a	^b	^d
	Unstiffened d'/t_w	$0.64\sqrt{E_s/F_{yw}}$	^b	$0.64\sqrt{E_s/F_{yw}}$
Flexural links	b'/t_f	$0.64\sqrt{E_s/F_{yf}}$	$1.00\sqrt{E_s/F_{yf}}$	$0.64\sqrt{E_s/F_{yf}}$
	Stiffened d'/t_w	^a	^b	^d
	Unstiffened d'/t_w	$0.64\sqrt{E_s/F_{yw}}$	^b	$0.64\sqrt{E_s/F_{yw}}$

^aAISC does not consider stiffened HSS walls.

^bStiffener spacing equations rather than compactness ratio limits for webs were derived in Berman and Bruneau (2007).

^cThe stiffened web compactness limit was found by limiting the stiffener spacing to the practical lower bound of approximately $0.4d'$.

^dFinite-element results indicate that stiffeners do not enhance the performance of intermediate or flexural links because flange buckling typically occurs prior web buckling.

and flexural links be limited to that for unstiffened shear links. This results from the observation that stiffeners do not enhance the performance of intermediate or flexural links because flange buckling typically occurs prior web buckling. Stiffeners in these cases only change the wavelength of flange buckling, which has only a slight impact on the limit rotation. The stiffener spacing equation was found to be adequate and remains unchanged from that derived in Berman and Bruneau (2007) and given in Eq. (6), although it is only recommended for shear links with web compactness values between $0.64\sqrt{E_s/F_{yw}}$ and $1.67\sqrt{E_s/F_{yw}}$.

It was also observed in Part A of the study that all flexural links with flange compactness ratios less than or equal to 24.0, for any of the four web compactness ratios considered, achieved their target rotation. As a result, the limit flange compactness ratio for flexural links could be increased to $1.00\sqrt{E_s/F_{yf}}$. However, for simplicity, and because they are not commonly used, the compactness ratio requirements for flexural links are recommended to be the same as those for shear and intermediate links, namely, $0.64\sqrt{E_s/F_{yf}}$. Further, it appears that stiffening the flange has no consequential effect on the maximum rotation capacity of links where flange buckling controls, so web only stiffeners were required are adequate. Finally, as mentioned earlier, it may be possible to allow larger flange compactness ratios for shear and intermediate links if the limit plastic rotation was made a function of both the link length and flange compactness ratio. The corresponding recommended rotation limits if one considered using such an with increased complexity are presented by Berman and Bruneau (2006). These are not included in the proposed design requirements here for simplicity and to keep the proposed requirements for rectangular links similar to the current requirements for WF links.

Parametric Study Part B: Setup

As tubular links may be fabricated with four plates welded together, hybrid cross sections where the yield stresses of the webs and flanges are different could be used advantageously. Further, the increased use of low yield point and high performance steels indicates a practical need for verifying the revised design requirements for a range of possible yield stresses. Part B of the finite element parametric study will therefore investigate tubular links with cross-sectional properties near the revised limits of Table 4 while also incorporating different yield stresses for both the webs and flanges.

Three yield stresses are considered for this part of the study, namely, 250 MPa (36 ksi), 345 MPa (50 ksi), and 450 MPa (65 ksi) as these are representative of some of the steels currently available. True stress versus true strain curves for the material models are shown in Fig. 7. The same normalized link lengths used in Part A of the study were used in Part B (i.e., ρ values of 1.2, 1.6, 2.1, and 3.0). Link web and flange compactness ratios for Part B of the parametric study were within 1% of the revised limits from Table 4. All links had flange compactness ratios near $0.64\sqrt{E_s/F_{yf}}$ and links with web compactness ratios near both $0.64\sqrt{E_s/F_{yw}}$ and $1.67\sqrt{E_s/F_{yw}}$ were considered. Links with the larger web compactness ratio were stiffened according to Eq. (6). For completeness, intermediate and flexural links with the larger web compactness ratio were developed, although these are outside the proposed design requirements. All combinations of parameters (i.e., 4 normalized lengths, 3 web yield stresses, 3 flange yield stresses, and 2 web compactness ratios) were considered, resulting in 72 links in Part B of the parametric study.

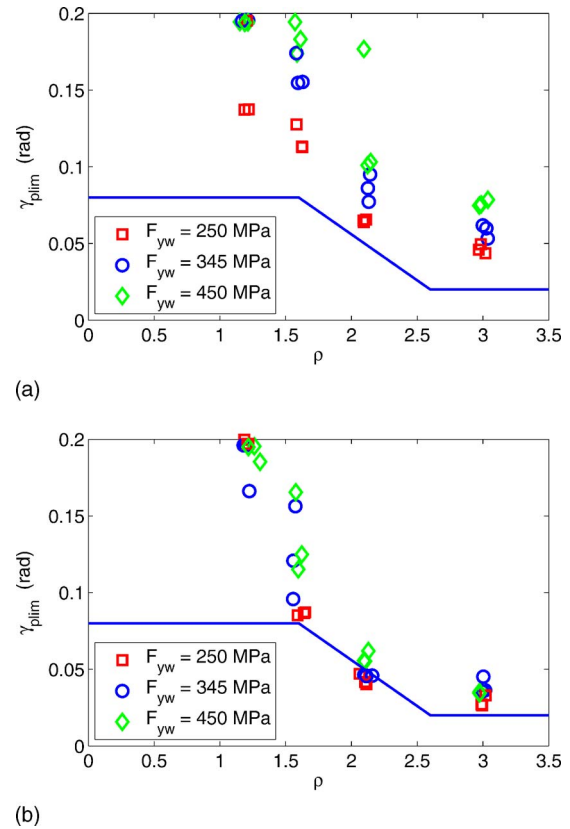


Fig. 12. Limit plastic rotations for Part B links (a) unstiffened with lower web compactness ratio; (b) stiffened with larger web compactness ratio

Parametric Study Part B: Results

Figs. 12(a and b) show limit plastic rotation versus link length for unstiffened links (those with web compactness near $0.64\sqrt{E_s/F_{yw}}$) and stiffened links (those with web compactness near $1.67\sqrt{E_s/F_{yw}}$), respectively, both grouped by web yield stress.

As shown in Figs. 12(a and b) all unstiffened links (i.e., those with web compactness near $0.64\sqrt{E_s/F_{yw}}$) reached their target rotations, and all stiffened links, except some at the intermediate length of 2.1, reached their target rotations. The links that did not reach their target rotation in Fig. 12(b) are intermediate links that do not satisfy the proposed design requirements. These links were included for comparison purposes, and have the stiffened webs with a compactness ratio near $1.67\sqrt{E_s/F_{yw}}$, which is only allowed for shear links. Therefore, as all Part B links that satisfied the proposed design requirements met their target rotations, these requirements appear to be satisfactory for the range of web and flange yield strengths considered.

Overstrength of Tubular Links

Determination of the maximum shear force a link can deliver is necessary to ensure capacity design of surrounding framing. Richards (2004) observed that as WF links get shorter the flanges begin to share some of the applied shear. This results in ultimate shear strengths exceeding what would be expected considering only strain hardening. Therefore, they derived a method for approximating the ultimate shear strength of WF links that depends on the web plastic shear, the shear resisted by the flanges, and the

normalized link length. In Berman and Bruneau (2005a), that method was modified to be applicable to links with tubular cross sections.

Richards (2004) presented the ultimate link shear strength in the form:

$$V_{ult} = \Omega R_y V_{pt} \quad (8)$$

where V_{pt} =total plastic shear force (considering the flange shear as appropriate); Ω =cyclic hardening factor defined in the following; and R_y =ratio of mean to nominal material yield stress as given in AISC Seismic Provisions. The shear carried by the flanges of a tubular link, V_f , can be found from (Berman and Bruneau 2005a)

$$V_f = \frac{F_y b t_f^2}{2e} - \frac{F_y t_w^2 e}{8b} \quad (9)$$

and the total plastic shear force, V_{pt} , is

$$V_{pt} = 0.6 F_{yw} t_w (d - 2t_f) + 2V_f \quad (10)$$

Note that Eq. (9) assumes that the webs and flanges have the same yield strength, F_y , and that if the web and flange yield strengths do differ, an average value may be used.

Richards then suggests that the cyclic hardening parameter, Ω , should vary with link length as

$$\Omega = 1.44, \quad \rho \leq 1.6$$

$$\Omega = 1.44 - 0.4(\rho - 1.6), \quad 1.6 < \rho \leq 2.6$$

$$\Omega = 2.7/\rho, \quad \rho \geq 2.6 \quad (11)$$

where the 2.7 value in the last expression in Eq. (11) is found by assuming that the maximum moment that can develop is $1.35M_p$ (less than the 1.44 used for shear links due to flange buckling limiting the strength of flexural links and the fact that stiffeners do not prevent this failure mode) and employing the link shear-moment relationship for flexural links ($V=2M_p/e$).

Figs. 13(a and b) show the ultimate link shear obtained in the finite element analyses of Part A links normalized by V_{ult} as defined earlier, versus normalized link length for unstiffened and stiffened links, respectively. The solid line in Figs. 13(a and b) indicates the curve for the cyclic hardening factor as given by Eq. (11) multiplied by an R_y value of 1.1 (appropriate for the A572 Grade 50 steel considered here). It appears that the overstrength equations proposed by Richards (2004) for WF links and modified in Berman and Bruneau (2005a) for application to tubular links, adequately estimates the ultimate link shear force (from which the maximum link end moment may be found). Similar agreement with the results from Part B of the parametric study was observed (Berman and Bruneau 2006). This procedure seems to provide a more uniform level of safety relative to a single valued overstrength factor, in terms of capacity protection of structural members outside the link, for all link lengths and yielding types. The points at small normalized link lengths that are above this proposed overstrength may suffer flange fracture prior to reaching the large overstrengths obtained from the finite element analyses, but further investigation of this is necessary before further changes are considered to address these extremes. Overstrength will be experimentally investigated in the companion paper (Berman and Bruneau 2008) to assess whether the results predicted here for the cyclic hardening factor applicable to rectangular links are appropriate.

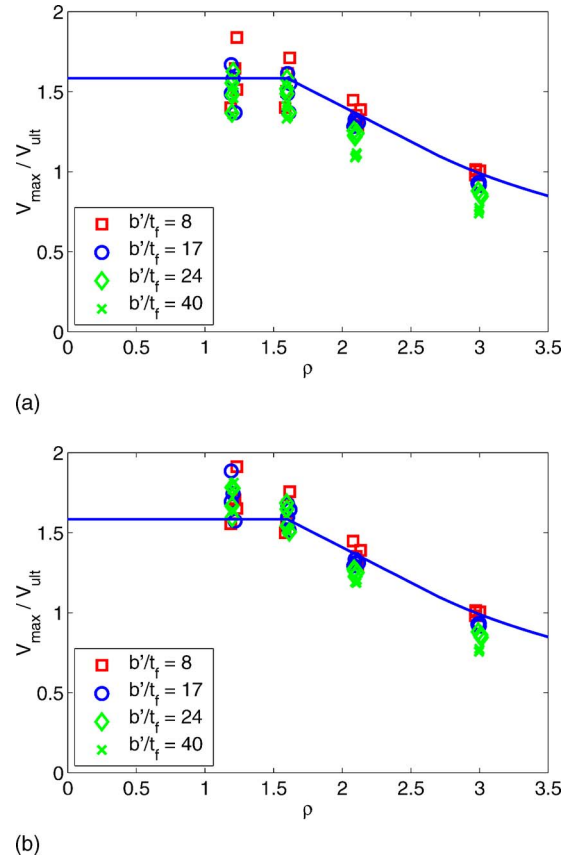


Fig. 13. Link overstrength for Part A links: (a) unstiffened links; (b) stiffened links

Conclusions

A finite element parametric study consisting of over 200 models of EBF links with tubular cross sections has been conducted. The study investigated a wide range of link geometries and properties, including web and flange compactness ratios, the presence of web stiffeners, link length, and web and flange yield strength. Results of the parametric study lead to the following recommendations for compactness ratio limits for tubular cross sections used as links in EBFs, which are also shown graphically in a design space in Fig. 14:

- All tubular links should have $b'/t_f \leq 0.64\sqrt{E_s/F_{yf}}$;
- Shear links ($\rho \leq 1.6$) should have $d'/t_w \leq 1.67\sqrt{E_s/F_{yw}}$ and those with $d'/t_w > 0.64\sqrt{E_s/F_{yw}}$ should have stiffeners with spacing, a , satisfying Eq. (6); and
- Intermediate and flexural links ($\rho > 1.6$) should have $d'/t_w \leq 0.64\sqrt{E_s/F_{yw}}$.

Analysis results indicate that if these compactness ratio recommendations are satisfied, tubular links will be able to achieve the maximum rotation levels in the AISC Seismic Provisions for links with WF cross sections. This conclusion was also verified by analyses for tubular links with webs and flanges having different yield strengths, in the range of 250–450 MPa. Additionally, a procedure for determining the ultimate strength of tubular links, based on a similar procedure derived by others for WF links, was shown to reasonably approximate the overstrength of the tubular links considered in the analyses. A companion paper, Berman and Bruneau (2008), describes the results of an experimental program to verify the above-presented design recommendations. Addi-

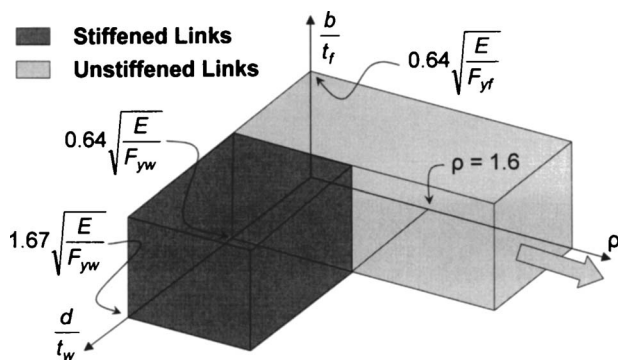


Fig. 14. Proposed design space for web and flange compactness ratios versus normalized link length

tional information on both the analytical and experimental work can be found in Berman and Bruneau (2006).

Acknowledgments

This research was conducted by the State University of New York at Buffalo and was supported by the Federal Highway Administration under Contract No. DTFH61-98-C-00094 the Multidisciplinary Center for Earthquake Engineering Research. However, any opinions, findings, conclusions, and recommendations presented in this paper are those of the writers and do not necessarily reflect the views of the sponsors.

References

AISC. (2002). *Seismic provisions for structural steel buildings*, Chicago.

AISC. (2005). *Seismic provisions for structural steel buildings*, Chicago.

Applied Technology Council (ATC). (1992). "Guidelines for seismic testing of components of steel structures." *Rep. No. 24*, Redwood City, Calif.

Berman, J. W., and Bruneau, M. (2005a). "Approaches for the seismic retrofit of braced steel bridge piers and proof-of-concept testing of a laterally stable eccentrically braced frame." *Technical Rep. No. MCEER-05-0004*, Multidisciplinary Center for Earthquake Engineering Research, Buffalo, N.Y.

Berman, J. W., and Bruneau, M. (2005b). "Supplemental system retrofit considerations for braced steel bridge piers." *J. Earthquake Eng.*, 34(4,5), 497–517.

Berman, J. W., and Bruneau, M. (2006). "Further development of tubular eccentrically braced frame links for the seismic retrofit of braced steel truss bridge piers." *Technical Rep. No. MCEER-06-0006*, Multidisciplinary Center for Earthquake Engineering Research, Buffalo, N.Y.

Berman, J. W., and Bruneau, M. (2007). "Experimental and analytical investigation of tubular links for eccentrically braced frames." *Eng. Struct.*, 29(8), 1929–1938.

Berman, J. W., and Bruneau, M. (2008). "Tubular links for eccentrically braced frames. II: Experimental verification." *J. Struct. Eng.*, 134(5), 702–712.

Dusicka, P., Itani, A. M., and Buckle, I. G. (2002). "Cyclic behavior of shear links and tower shaft assembly of San Francisco-Oakland Bay Bridge Tower." *Technical Rep. No. CCEER 02-06*, Center for Civil Engineering Earthquake Research, Univ. of Nevada, Reno, Reno, Nev.

Engelhardt, M. D., and Popov, E. P. (1992). "Experimental performance of long links in eccentrically braced frames." *J. Struct. Eng.*, 118(11), 3067–3088.

Hibbit, Karlsson, and Sorensen, Inc. (HKS). (2001). *ABAQUS standard user's manual*, Pawtucket, R.I.

Hjelmstad, K. D., and Popov, E. P. (1983). "Cyclic behavior and design of link beams." *J. Struct. Eng.*, 109(10), 2387–2403.

Hjelmstad, K. D., and Popov, E. P. (1984). "Characteristics of eccentrically braced frames." *J. Struct. Eng.*, 110(2), 340–353.

Itani, A. M. (1997). "Cyclic behavior of Richmond-San Rafael Tower links." *Technical Rep. No. CCEER 97-4*, Center for Civil Engineering Earthquake Research, Univ. of Nevada, Reno, Nev.

Kasai, K., and Popov, E. P. (1986a). "General behavior of WF steel shear link beams." *J. Struct. Eng.*, 112(2), 362–382.

Kasai, K., and Popov, E. P. (1986b). "Study of seismically resistant eccentrically braced steel frame systems." *Rep. No. UCB/EERC-86/01*, Earthquake Engineering Research Center, College of Engineering, Univ. of California, Berkeley, Calif.

Kaufmann, E. J., Metrovich, B., and Pense, A. W. (2001). "Characterization of cyclic inelastic strain behavior on properties of A572 Gr.50 and A913 Gr. 50 rolled sections." *ATLSS Rep. No. 01-13*, National Center for Engineering Research on Advanced Technology for Large Structural Systems, Lehigh Univ., Bethlehem, Pa.

Malley, J. O., and Popov, E. P. (1984). "Shear links in eccentrically braced frames." *J. Struct. Eng.*, 110(9), 2275–2295.

MathWorks. (1999). *MatLab function reference*, Natick, Mass.

Okazaki, T., Arce, G., Ryu, H. C., and Engelhardt, M. D. (2005). "Experimental study of local buckling, overstrength, and fracture of links in eccentrically braced frames." *J. Struct. Eng.*, 131(10), 1526–1535.

Okazaki, T., Engelhardt, M. D., Nakashima, M., and Suita, K. (2006). "Experimental performance of link-to-column connections in eccentrically braced frames." *J. Struct. Eng.*, 132(8), 1201–1211.

Popov, E. P., and Bertero, V. V. (1980). "Seismic analysis of some steel building frames." *J. Engrg. Mech. Div.*, 106(1), 75–92.

Richards, P. (2004). "Cyclic stability and capacity design of steel eccentrically braced frames." Ph.D. dissertation, Univ. of California, San Diego.

Richards, P., and Uang, C. M. (2005). "Effect of flange width-thickness ratio on eccentrically braced frames link cyclic rotation capacity." *J. Struct. Eng.*, 131(10), 1546–1552.

Richards, P., and Uang, C. M. (2006). "Testing protocol for short links in eccentrically braced frames." *J. Struct. Eng.*, 132(8), 1183–1191.

Ricles, J. M., and Popov, E. P. (1989). "Composite action in eccentrically braced frames." *J. Struct. Eng.*, 115(8), 2046–2066.

Roeder, C. W., and Popov, E. P. (1978a). "Cyclic shear yielding of wide-flange beams." *J. Engrg. Mech. Div.*, 104(4), 763–780.

Roeder, C. W., and Popov, E. P. (1978b). "Eccentrically braced steel frames for earthquakes." *J. Struct. Div.*, 104(3), 391–412.

Structural Engineers Association of California, Applied Technology Council, and Consortium of Universities for Research in Earthquake Engineering (SAC). (1997). "Advisory No. 1—Supplement to FEMA-267A: Evaluation, repair, modification and design of welded steel moment frame structures (interim guidelines)." *FEMA-267A*, Sacramento, Calif.